CellPress

Chemistry & Biology
Article

Intracellular Calcium Levels Determine Differential Modulation of Allosteric Interactions within G Protein-Coupled Receptor Heteromers

Gemma Navarro,[1,*] David Aguinaga,[1] Estefania Moreno,[1] Johannes Hradsky,[2] Pasham P. Reddy,[2] Antoni Cortés,[1] Josefa Mallol,[1] Vicent Casadó,[1] Marina Mikhaylova,[2,3] Michael R. Kreutz,[2] Carme Lluís,[1] Enric I. Canela,[1,6] Peter J. McCormick,[1,4,6] and Sergi Ferré[5,6,*]

[1]Department of Biochemistry and Molecular Biology, Faculty of Biology, University of Barcelona, Centro de Investigación Biomédica en Red Sobre Enfermedades Neurodegenerativas and Institute of Biomedicine of the University of Barcelona (IBUB), Barcelona 08028, Spain
[2]Research Group Neuroplasticity, Leibniz-Institute for Neurobiology, Magdeburg 39118, Germany
[3]Cell Biology, Utrecht University, Utrecht 3584, the Netherlands
[4]School of Pharmacy, University of East Anglia, Norwich NR4 7TJ, UK
[5]Integrative Neurobiology Section, National Institute on Drug Abuse, Intramural Research Program, Department of Health and Human Services, National Institutes of Health, Baltimore, MD 21224, USA
[6]Co-senior author
*Correspondence: dimartts@hotmail.com (G.N.), sferre@intra.nida.nih.gov (S.F.)
http://dx.doi.org/10.1016/j.chembiol.2014.10.004

SUMMARY

The pharmacological significance of the adenosine A_{2A} receptor (A_{2A}R)-dopamine D_2 receptor (D_2R) heteromer is well established and it is being considered as an important target for the treatment of Parkinson's disease and other neuropsychiatric disorders. However, the physiological factors that control its distinctive biochemical properties are still unknown. We demonstrate that different intracellular Ca^{2+} levels exert a differential modulation of A_{2A}R-D_2R heteromer-mediated adenylyl-cyclase and MAPK signaling in striatal cells. This depends on the ability of low and high Ca^{2+} levels to promote a selective interaction of the heteromer with the neuronal Ca^{2+}-binding proteins NCS-1 and calneuron-1, respectively. These Ca^{2+}-binding proteins differentially modulate allosteric interactions within the A_{2A}R-D_2R heteromer, which constitutes a unique cellular device that integrates extracellular (adenosine and dopamine) and intracellular (Ca^{+2}) signals to produce a specific functional response.

INTRODUCTION

G protein-coupled receptors (GPCR) heteromers are defined as macromolecular complexes composed of at least two functional receptor units with biochemical properties that are different from those of its individual receptors (Ferré et al., 2009). Allosteric mechanisms are responsible for a multiplicity of unique pharmacological properties of GPCR heteromers (Ferré et al., 2014). One of the most reproduced allosteric modulations in a GPCR heteromer is an antagonistic interaction by which adenosine A_{2A} receptor (A_{2A}R) agonists decrease the affinity of dopamine D_2 receptor (D_2R) agonists in the A_{2A}R-D_2R heteromer (Ferré et al., 1991). A_{2A}R-D_2R heteromers were one of the first GPCR heteromers detected in the brain. They are localized in the striatum, in the GABAergic striato-pallidal neurons, where they play a seminal role controlling basal ganglia function and dysfunction (Ferré et al., 2011).

Apart from modulation of ligand affinity, GPCR oligomers enable ligands to exert different intrinsic efficacy (power of the agonist to induce a functional response independent of its affinity for the receptor) for different signaling pathways (functional selectivity) (Ferré et al., 2014). Thus, allosteric changes in the functional response of an agonist can be mediated by changes in affinity and/or intrinsic efficacy. This principal can be observed in the A_{2A}R-D_2R heteromer, where a decrease in D_2R agonist affinity could not alone explain the ability of A_{2A}R agonists to abolish the decrease in excitability of GABAergic striato-pallidal neurons induced by high concentrations of D_2R agonists, sufficient to overcome their decreased affinity (Azdad et al., 2009).

A_{2A}R and D_2R couple preferentially to $G_{s/olf}$ and G_i proteins, respectively, and several studies have reported an antagonistic interaction reciprocal to the A_{2A}R-D_2R allosteric modulations, the ability of D_2R ligands to potently inhibit A_{2A}R agonist-mediated adenylyl-cyclase (AC) activation (Kull et al., 1999; Hillion et al., 2002). It is not known if this canonical interaction between G_s- and G_i-mediated signaling pathways takes place in the frame of the A_{2A}R-D_2R heteromer, as suggested for dopamine D_1-D_3 receptor heteromers (Guitart et al., 2014), or if it depends on separate receptor populations (Ferré et al., 2011). But if it is a property of the A_{2A}R-D_2R heteromer, we do not know the physiological factors that modulate these reciprocal interactions, determining the final neuronal response.

Intracellular Ca^{2+} levels are a physiological factor that modulates neuronal activity and GPCR function. The Ca^{2+}-binding protein calmodulin (CaM) has been shown to interact and modulate A_{2A}R and D_2R function in the A_{2A}R-D_2R heteromers, but without altering the allosteric interactions between A_{2A}R and D_2R ligands (Navarro et al., 2009; Ferré et al., 2010). CaM is an ancestor of a superfamily of Ca^{2+}-binding proteins, which includes neuronal members classified in neuronal Calcium Binding

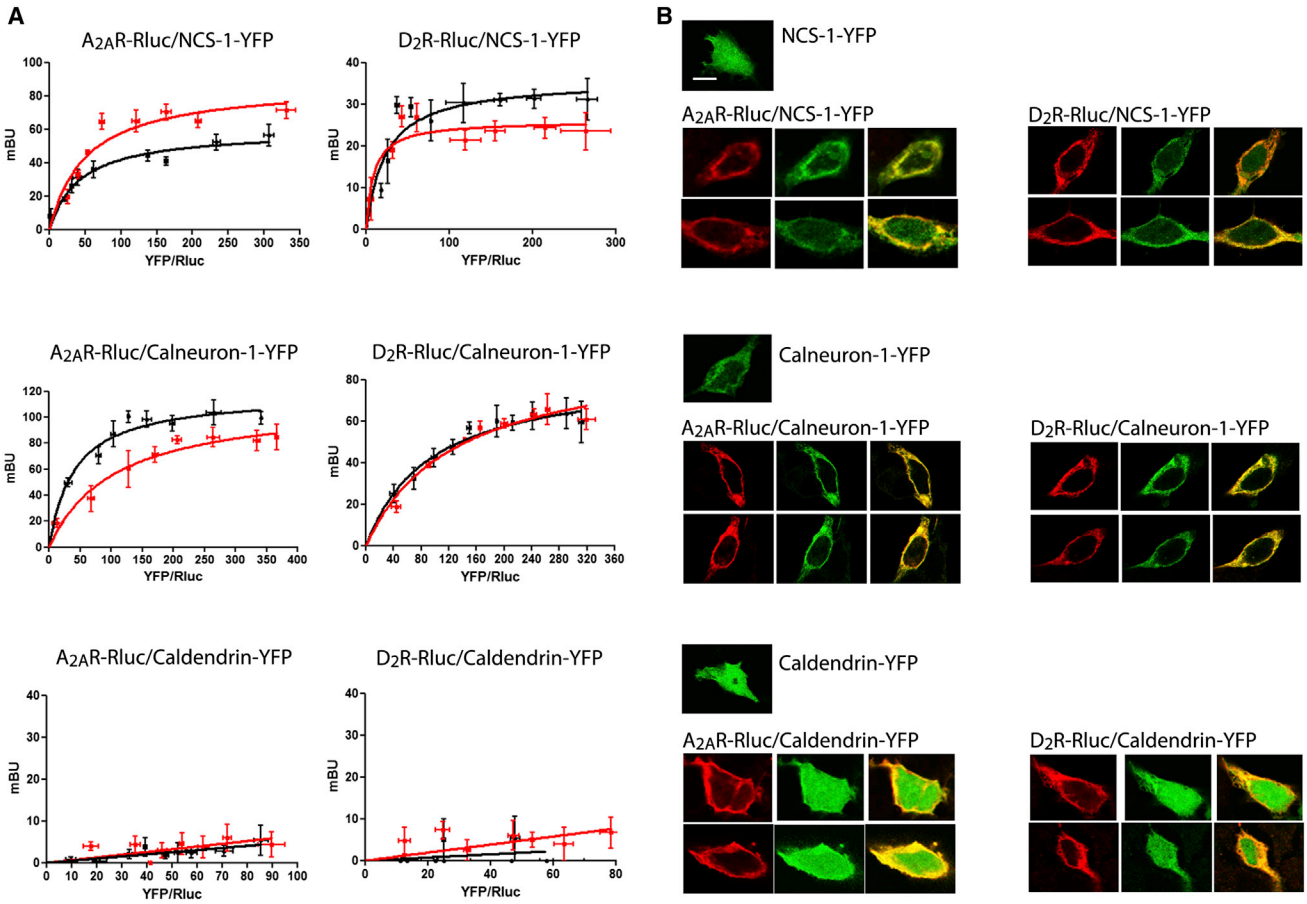

Figure 1. NCS-1 and Calneuron-1, but Not Caldendrin, Interact with $A_{2A}R$ and D_2R

(A) BRET saturation experiments in HEK293T cells transfected with $A_{2A}R$-Rluc cDNA (0.2 μg; left graphs) or D_2R-Rluc cDNA (0.4 μg; right graphs) and increasing amounts of NCS-1-YFP cDNA (0.2 to 0.8 μg; top graphs), calneuron-1-YFP cDNA (0.4 to 1.2 μg; middle graphs), or caldendrin-YFP cDNA (0.2 to 1 μg; bottom graphs), in the absence (black curves) or in the presence (red curves) of 1 μM ionomycin. The relative amount of BRET is given as a function of 1,000 × the ratio between the fluorescence of the acceptor (YFP) and the luciferase activity of the donor (Rluc). BRET is expressed as miliBRET units (mBU) and is given as means ± SEM of five to seven different experiments grouped as a function of the amount of BRET acceptor.

(B) Confocal microscopy images of HEK293T cells transfected with NCS-1-YFP cDNA (0.5 μg; top panels), calneuron-1-YFP cDNA (0.7 μg; middle panels), or caldendrin-YFP cDNA (0.5 μg; bottom panels), cotransfected or not with $A_{2A}R$-RLuc cDNA (0.4 μg; left panels) or D_2R-Rluc cDNA (0.6 μg; right panels). Receptors were identified by immunocytochemistry (red) and proteins fused to YFP were identified by its own fluorescence (green). Colocalization is shown in yellow in merge figures. Scale bar, 10 μm.

Proteins (CaBPs, such as caldendrin and calneuron-1) and the Neuronal Calcium Sensor (NCS) proteins (such as NCS-1) (Mikhaylova et al., 2011). NCS-1, caldendrin, and calneuron-1 have overlapping expression in the brain and have been shown to dramatically modify GPCR function (Mikhaylova et al., 2009). NCS-1 is also known to interact and modify the function of $A_{2A}R$ and D_2R (Kabbani et al., 2002; Saab et al., 2009; Navarro et al., 2012). We therefore studied if neuronal Ca^{2+}-binding proteins could provide the pursued modulators of the allosteric interactions in the $A_{2A}R$-D_2R heteromers.

RESULTS

NCS-1 and Calneuron-1 Directly Interact with $A_{2A}R$-D_2R Heteromers

Bioluminescence resonance energy transfer (BRET) experiments were performed in HEK293T cells in which one of the receptors is fused to the bioluminescent protein *Renilla* Luciferase (RLuc) and the Ca^{2+}-binding protein to a yellow fluorescent protein (YFP). Protein interactions were detected by saturable BRET curves in cells expressing a constant amount of $A_{2A}R$-Rluc or D_2R-Rluc and increasing amounts of NCS-1-YFP or calneuron-1-YFP (Figure 1A, top and middle graphs). $BRET_{max}$ and $BRET_{50}$ values were, respectively, 59.6 ± 4 mBU and 42.4 ± 9 for the pair $A_{2A}R$-Rluc-NCS1-1-YFP; 35.8 ± 4 mBU and 23.4 ± 5 for the pair D_2R-Rluc-NCS-1-YFP; 118.1 ± 7 mBU and 40.5 ± 7 for the pair $A_{2A}R$-Rluc-calneuron-1-YFP; and 51.9 ± 10 mBU and 25.7 ± 7 for the pair D_2R-Rluc-calneuron-1-YFP. Very low and linear BRET was detected in cells expressing a constant amount of $A_{2A}R$-Rluc or D_2R-Rluc and increasing amounts of caldendrin-YFP (Figure 1A, bottom graph), showing the inability of caldendrin to interact with $A_{2A}R$ or D_2R, and the specificity of NCS-1 and calneuron-1 interactions. Increasing intracellular Ca^{2+} levels with ionomycin produced noticeable changes in

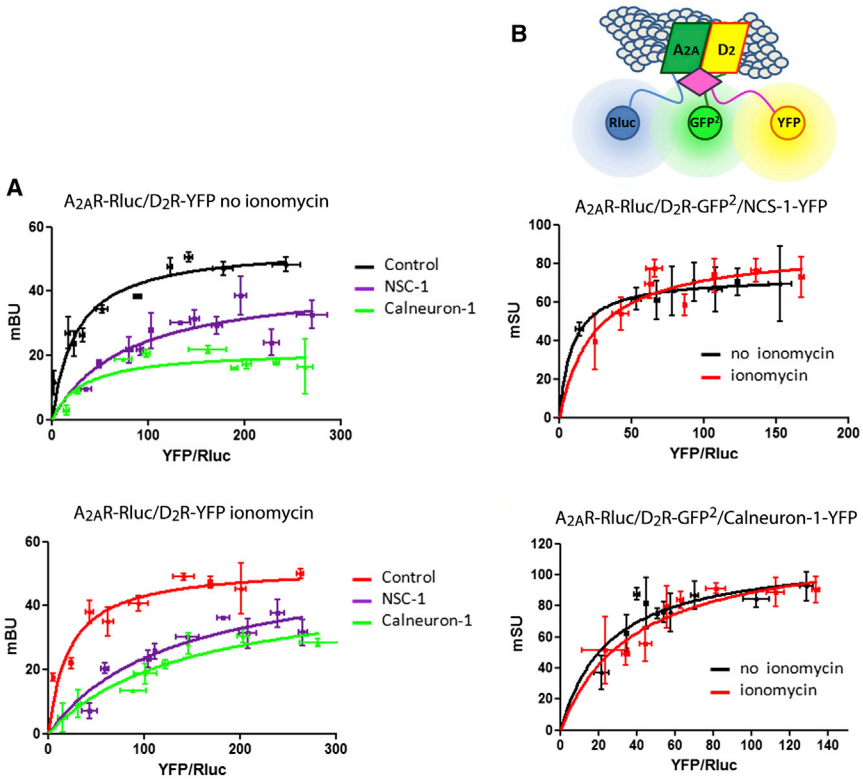

Figure 2. NCS-1 and Calneuron-1 Interact with $A_{2A}R$-D_2R Heteromers

(A) BRET saturation experiments in HEK293T cells transfected with $A_{2A}R$-Rluc cDNA (0.2 μg) and increasing amounts of D_2R-YFP cDNA (0.1 to 1 μg) with or without NCS-1 cDNA (0.7 μg) or calneuron-1 cDNA (1 μg), in the absence (top graph) or in the presence (bottom graph) of 1 μM ionomycin.

(B) Sequential resonance energy transfer (SRET) saturation experiments in HEK293T cells transfected with $A_{2A}R$-Rluc cDNA (0.3 μg), D_2R-GFP^2 cDNA (0.4 μg), and increasing amounts of NCS-1-YFP cDNA (0.3 to 0.8 μg; top graph) or calneuron-1-YFP cDNA (0.5 to 1.5 μg; bottom graph), in the absence (black curves) or presence (red curves) of 1 μM ionomycin. Scheme shows SRET with the sequential BRET (Rluc as donor and GFP^2 as acceptor) and FRET (GFP^2 as donor and YFP as acceptor) processes. BRET or SRET are expressed as miliBRET or miliSRET units (mBU, mSU), respectively, and given as a function of 1,000 × the ratio between the fluorescence of the acceptor (YFP) and the luciferase activity of the donor (Rluc). Values are means ± SEM of six to eight different experiments.

the BRET curves for the pairs $A_{2A}R$-Rluc-NCS-1-YFP, D_2R-Rluc-NCS-1-YFP, and A_{2A}-Rluc-calneuron-1-YFP (Figure 1A, top and middle graphs), indicating that Ca^{2+} binding to NCS-1 or calneuron-1 induces structural changes in the respective complexes. In accordance with the BRET data, the intracellular distribution of NCS-1 dramatically changed to a plasma membrane distribution after $A_{2A}R$ or D_2R coexpression (Figure 1B, top panel). Calneuron-1 expressed alone showed a membrane localization that was maintained in the presence of $A_{2A}R$ or D_2R with a high degree of colocalization (Figure 1B, middle panel). Caldendrin did not change its intracellular distribution when coexpressed with either receptor (Figure 1B, bottom panel).

Heteromers were detected by saturable BRET curves in cells expressing a constant amount of $A_{2A}R$-Rluc and increasing amounts of D_2R-YFP in the absence or in the presence of ionomycin (Figure 2A). Coexpression of calneuron-1 or NCS-1 induced structural changes in the heteromer detected as changes in the BRET curve shape (Figure 2A). This suggested oligomerization between $A_{2A}R$-D_2R heteromers and the Ca^{2+}-binding proteins, which was further supported by sequential resonance energy transfer (SRET) experiments (Carriba et al., 2008). Rluc was fused to $A_{2A}R$ to act as a BRET donor, GFP^2 was fused to D_2R to act as a BRET acceptor and as a FRET donor, and YFP was fused to NCS-1 or to calneuron-1 to act as a FRET acceptor as diagrammed in Figure 2B (top scheme). In cells expressing a constant amount of $A_{2A}R$-Rluc and D_2R-GFP^2 and increasing amounts of NCS-1-YFP (Figure 2B, middle graph) or calneuron-1-YFP (Figure 2B, bottom graph), a positive SRET saturation curve was obtained in the absence (black curves) or in the presence (red curves) of ionomycin, with a $SRET_{max}$ of 73.3 ± 2 mSU and $SRET_{50}$ of 8.9 ± 2 or $SRET_{max}$ of 88.2 ± 9 mSU and $SRET_{50}$ of 24.1 ± 6 for the $A_{2A}R$-D_2R-NCS-1 complex in the absence or in the presence of ionomycin, respectively, and a $SRET_{max}$ of 113.2 ± 14 mSU and $SRET_{50}$ of 25.1 ± 7 or $SRET_{max}$ of 122.6 ± 15 mSU and $SRET_{50}$ of 38.5 ± 10 for the $A_{2A}R$-D_2R-calneuron-1 complex in the absence or in the presence of ionomycin, respectively. Therefore, both NCS-1 and calneuron-1 bind to $A_{2A}R$-D_2R heteromers independently of the presence of Ca^{2+}.

To investigate if membrane localization of the Ca^{2+}-binding proteins, mediated by C-terminal transmembrane domain in calneuron-1 and N-terminal myristoylation of NSC-1 (Hradsky et al., 2011), are necessary for the interaction with $A_{2A}R$ and D_2R, we used a calneuron-1 construct truncated in its C terminus (calneuron-1ΔCT) (Hradsky et al., 2011) and an N-terminal myristoylation-deficient NCS-1 mutant. No BRET signal was detected in cells expressing $A_{2A}R$-Rluc or D_2R-Rluc and increasing amounts of mutant calneuron-YFP (Figure S1A, top graphs, available online). Very low and linear BRET values were also obtained in cells expressing $A_{2A}R$-Rluc or D_2R-Rluc and increasing amounts of mutant NCS1-YFP (Figure S1A, bottom graphs).

NCS-1 and Calneuron-1 Compete for the Binding to $A_{2A}R$ and D_2R

Competition BRET experiments were performed in which energy transfer between $A_{2A}R$-Rluc-NCS-1-YFP was measured in the presence of increasing concentrations of calneuron-1 with or without ionomycin (Figure 3A, left graph). In both conditions, calneuron-1 dose-dependently lowered the energy transfer, indicating competition between both Ca^{2+}-binding proteins for $A_{2A}R$. Similar results were obtained with D_2R. NCS-1 reduced

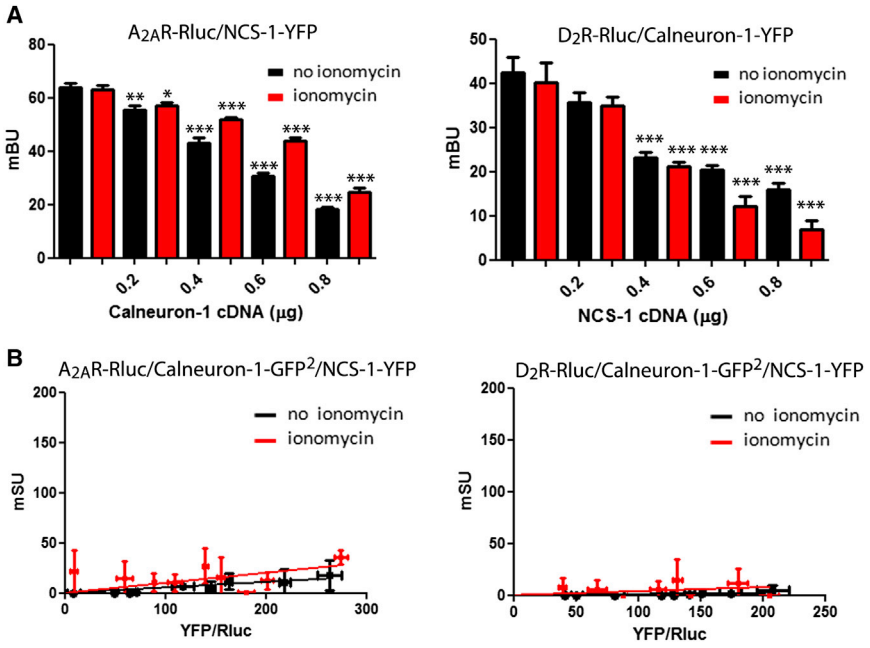

Figure 3. NCS-1 and Calneuron-1 Compete for Binding to $A_{2A}R$ and D_2R

(A) BRET competition experiments in HEK293T cells transfected with $A_{2A}R$-Rluc cDNA (0.2 μg) and NCS-1-YFP cDNA (0.7 μg) with increasing amounts of calneuron-1 cDNA (0.2 to 0.8 μg; left graph) or with D_2R-Rluc cDNA (0.3 μg) and calneuron-1-YFP cDNA (1 μg; right graph) with increasing amounts of NCS-1 cDNA (0.2 to 0.8 μg, right graph) in the absence (black bars) or presence (red bars) of 1 μM ionomycin. BRET, expressed as miliBRET units (mBU), is given as means ± SEM of six to eight different experiments. One-way ANOVA followed by post hoc Dunnett's multiple comparisons: *$p < 0.05$, **$p < 0.01$, and ***$p < 0.001$ versus BRET in the absence of NCS-1 or calneuron-1.

(B) SRET in HEK293T cells transfected $A_{2A}R$-Rluc cDNA (0.2 μg; left graphs) or D_2R-Rluc cDNA (0.3 μg; right graph), and calneuron-1-GFP^2 cDNA (0.4 μg) and increasing amounts of NCS-1-YFP cDNA (0.2 to 0.8 μg) in the absence (black lines) or presence (red lines) of 1 μM ionomycin. The relative amount of SRET, expressed as miliSRET units (mSU), is given as a function of 1,000 × the ratio between the fluorescence of the acceptor (YFP) and the luciferase activity of the donor (Rluc). Values are means ± SEM of four to six different experiments.

the energy transfer between D_2R-Rluc and calneuron-1-YFP in the absence or presence of ionomycin (Figure 3A, right graph). Therefore, NCS-1 and calneuron-1 bind and compete for the same binding sites on $A_{2A}R$ and D_2R. In agreement, low and linear SRET curves were obtained in the absence or in the presence of ionomycin in cells expressing $A_{2A}R$-Rluc-calneuron-1-GFP^2-NCS-1-YFP or D_2R-Rluc-calneuron-1-GFP^2-NCS-1-YFP (Figure 3B).

BRET saturation values were significantly diminished when a mutant $A_{2A}R$ fused to Rluc in which the sequence $_{199}$RIFLAARRQ$_{207}$ (localized in the cytoplasm, at the end of TM5) was mutated to $_{199}$RIFLAAAAQ$_{207}$ ($A_{2A}R^{A205\text{-}A206}$ receptor) was coexpressed with either NCS-1-YFP or calneuron-1-YFP (Figure S1B). NCS-1 and calneuron-1 thus interact with the third intracellular loop (3IL) of $A_{2A}R$. This was confirmed by surface plasmon resonance measurements showing the in vitro interaction between the Ca^{2+}-binding proteins and glutathione S-transferase (GST) fused to a peptide with the amino acid sequence corresponding to the third intracellular loop of the $A_{2A}R$ (GST-$A_{2A}R$-IL3) (Figure S2, top graphs). The sequence corresponding to amino acids 428–443 in the C-terminal domain of the D_2R has been involved in NCS-1 binding (Kabbani et al., 2002). In agreement, a complete loss of BRET was observed when a D_2R mutant lacking this sequence ($D_2R^{428–443}$) fused to Rluc was coexpressed with NCS-1-YFP (Figure S1C, top left graph). In addition, a significant but partial modification of the D_2R-Rluc/calneuron-1 BRET saturation curve was obtained with $D_2R^{428–443}$-Rluc (Figure S1C, top right graph). A partial modification of the D_2R-Rluc/calneuron-1 BRET saturation curve was also obtained with the short isoform of D_2R fused to Rluc ($D_{2S}R$-Rluc, which lacks an Arg-rich epitope in the middle of the 3IL of the long isoform) (Figure S1C, bottom right graph). On the other hand, no significant differences were observed between $D_{2S}R$-Rluc/NCS-1 BRET saturation curves (Figure S1C, bottom left graph). These results reinforce the assumption that the C-terminal domain of D_2R is sufficient for NCS-1 binding and indicate that both the C-terminal domain and the 3IL of D_2R are involved in calneuron-1 binding. The role of the D_2R C-terminal domain in the interaction with both Ca^{2+}-binding proteins was confirmed with surface plasmon resonance measurements using a peptide with the amino acid sequence of the C-terminal domain of the D_2R coupled to the biosensor (Figure S2, bottom graphs).

Differential Modulation by NCS-1 and Calneuron-1 of Allosteric Interactions within $A_{2A}R$-D_2R Heteromers

In HEK293T cells expressing $A_{2A}R$ alone or $A_{2A}R$ and D_2R, the $A_{2A}R$ agonist CGS 21680 (100 nM) induced ERK1/2 phosphorylation, which was completely blocked by the protein kinase A inhibitor H89 (Figure S3), indicating a G protein-cAMP-PKA-dependent $A_{2A}R$-mediated mitogen-activated protein kinase (MAPK) activation. In cells expressing $A_{2A}R$ and the D_2R, CGS 21680 and the D_2R agonist quinpirole (1 μM) induced a similar degree of ERK1/2 phosphorylation, in the presence or absence of ionomycin (Figure 4A, black bars). The absence of additive effect indicates the presence of moderate negative crosstalk, a negative allosteric interaction between both ligands within the $A_{2A}R$-D_2R heteromer. Similar effects were observed in cells expressing NCS-1, in the absence or in the presence of ionomycin, (Figure 4A, gray bars), as well as in cells expressing calneuron-1, but only in the absence of ionomycin (Figure 4A, left graph, white bars). In the presence of calneuron-1 and ionomycin, a strong negative crosstalk was observed, without an increase of ERK1/2 phosphorylation over basal level and with significantly lower values upon coadministration of CGS 21680 plus quinpirole compared with CGS 21680 alone (Figure 4A, right graph, white bars). As negative control, this effect was not observed when using the truncated mutant of calneuron-1, not able to bind to the $A_{2A}R$ or D_2R (Figure S4A). These results suggest that at high, but not low, intracellular levels of Ca^{2+},

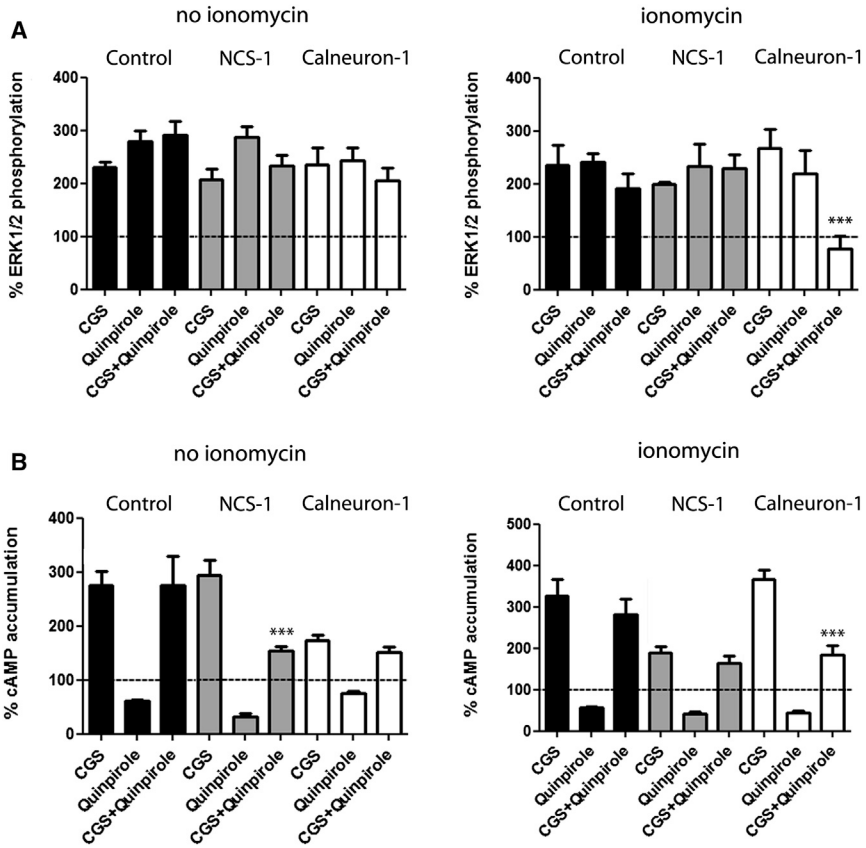

Figure 4. Modulation by NCS-1 and Calneuron-1 of $A_{2A}R$-D_2R Heteromer Signaling in Transfected Cells

(A) ERK1/2 phosphorylation in HEK293T cells transfected with $A_{2A}R$-Rluc cDNA (0.3 μg) and D_2R-YFP cDNA (0.5 μg) alone (black bars) or also transfected with NCS-1 cDNA (0.4 μg cDNA; gray bars) or calneuron-1 cDNA (0.6 μg; white bars) after administration of the $A_{2A}R$ agonist CGS 21680 (CGS, 100 nM), the D_2R agonist quinpirole (1 μM), or both, in the absence or presence of ionomycin (left and right graphs, respectively). ERK1/2 phosphorylation levels are expressed as a percentage over basal.

(B) Levels of cAMP in HEK293T cells transfected with $A_{2A}R$-Rluc cDNA (0.3 μg) and D_2R-YFP cDNA (0.5 μg) alone (black bars) or also transfected with NCS-1 cDNA (0.4 μg cDNA; gray bars) or calneuron-1 cDNA (0.6 μg; white bars) after administration of the $A_{2A}R$ agonist CGS 21680 (CGS, 100 nM), the D_2R agonist quinpirole (1 μM), or both, in the absence or presence of ionomycin (left and right graphs, respectively). Levels of cAMP after CGS alone or after CGS plus quinpirole are expressed as a percentage over basal; cAMP after quinpirole alone are expressed as percentage of decreases with respect to cAMP induced by forskolin (0.5 μM); basal and forskolin-induced cAMP were given as 100% and represented by a dotted line. Values are mean ± SEM of four to six different experiments. One-way ANOVA followed by post hoc Dunnett's multiple comparisons: ***$p < 0.001$ versus CGS 21680 treatment.

calneuron-1 selectively facilitates a reciprocal negative allosteric interaction between CGS-21680 and quinpirole at the level of MAPK signaling in the $A_{2A}R$-D_2R heteromer.

In HEK293T cells expressing $A_{2A}R$ and D_2R receptors, CGS 21680 (100 nM) increased cyclic AMP (cAMP) accumulation and quinpirole (1 μM) decreased forskolin-induced cAMP accumulation in the absence or in the presence of ionomycin (Figure 4B, black bars). However, quinpirole did not counteract CGS 21680-induced cAMP accumulation (Figures 4B, black bars), indicating the existence of a strong negative allosteric modulation by which CGS 21680 significantly decreases the intrinsic efficacy of quinpirole as inhibitor of AC signaling. This modulation was also observed in cells expressing calneuron-1 in the absence of ionomycin (Figure 4B, left graph, white bars) and in cells expressing NCS-1, but in the presence of ionomycin (Figure 4B, right graph, white bars). In contrast, quinpirole was able to reduce cAMP accumulation induced by CGS 21680 in cells expressing calneuron-1 in the presence of ionomycin (Figure 4B, right graph, white bars) and in cells expressing NCS-1 but in the absence of ionomycin (Figure 4B, left graph, gray bars). As negative controls, the ability of quinpirole to counteract cAMP accumulation induced by CGS 21680 in the presence of ionomycin and calneuron-1 was not detected in cells expressing mutants of $A_{2A}R$ or D_2R not able to bind calneuron-1 (Figure S4B, left graph). These results suggest binding of calneuron-1 to both receptors in the $A_{2A}R$-D_2R heteromer is necessary to exert its modulation. The ability of quinpirole to counteract cAMP accumulation induced by CGS 21680 in the presence of NCS-1 and in the absence of ionomycin was not observed in cells expressing $A_{2A}R$ and the D_2R mutant not able to bind NCS-1 (Figure S4B, right graph). But in contrast to calneuron-1, the effect was observed for heteromers constituted by wild-type D_2R and the $A_{2A}R$ mutant not able to bind NCS-1 (Figure S7B, right graph), indicating that binding of NCS-1 to D_2R, but not to the $A_{2A}R$, in the heteromer is sufficient to exert its modulation.

Ca^{2+} Levels Determine the Binding of NCS-1 and Calneuron-1 to $A_{2A}R$-D_2R Heteromers in Striatal Neurons

Proximity ligation assay (PLA) was used to confirm the expression of endogenous $A_{2A}R$-D_2R complexes in the primary cultures (Trifilieff et al., 2011). $A_{2A}R$-D_2R complexes could be observed as punctate red spots in neurons visualized by phase contrast and DAPI-stained nuclei (Figure 5A). The staining was observed in a high percentage of cells (>90%), but not in negative controls in which one of the primary antibodies was omitted (Figure S5, control neurons). To evaluate the role of endogenous NCS-1 and calneuron-1 in the modulation of $A_{2A}R$-D_2R heteromer function, ERK1/2 phosphorylation was determined in neurons transfected with small hairpin RNA (shRNA) against NCS-1 or calneuron-1 mRNA. Knockdown efficiency compared with control was verified by immunoblotting with specific antibodies against calneuron-1 or NCS1 and anti-tubulin antibodies as loading control (Figure S6). The transfection rate of calneuron-1 shRNA was analyzed by determination of GFP expression induced by

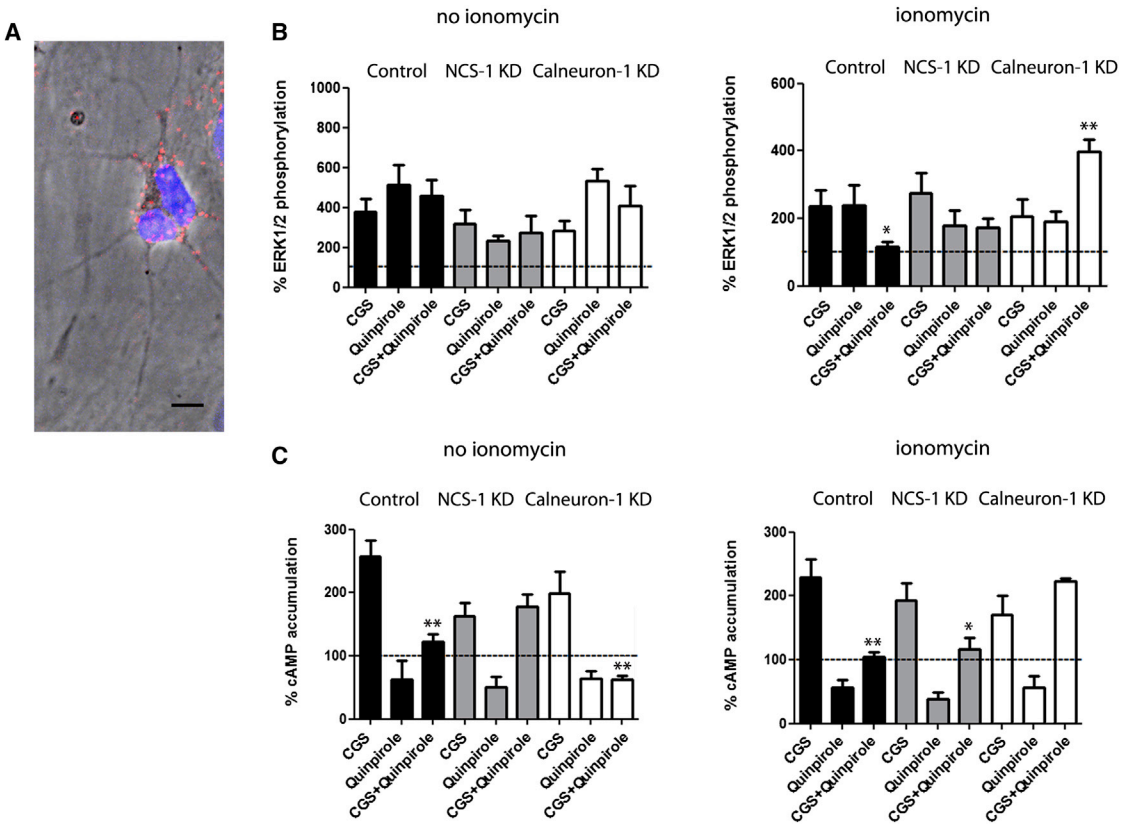

Figure 5. Modulation by NCS-1 and Calneuron-1 of $A_{2A}R$-D_2R Heteromer Signaling in Primary Cultures of Rat Striatal Neurons

(A) $A_{2A}R$-D_2R heteromers detected by proximity ligation assay and confocal microscopy images (superimposed sections) in rat striatal neurons in culture. $A_{2A}R$-D_2R heteromers are seen as red and cell nuclei in blue (Hoesch stain). Scale bars, 20 μm.

(B) ERK1/2 phosphorylation in striatal primary cultures not transfected or transfected with NCS-1 shRNA cDNA (1.5 μg; gray bars) or with calneuron-1 shRNA cDNA (1.5 μg; white bars) after administration of the $A_{2A}R$ agonist CGS 21680 (CGS, 100 nM), the D_2R agonist quinpirole (1 μM), or both, in the absence or presence of ionomycin (left and right graphs, respectively). ERK1/2 phosphorylation levels are expressed as a percentage over basal.

(C) Levels of cAMP in striatal primary cultures not transfected or transfected with NCS-1 shRNA cDNA (1.5 μg; gray bars) or with calneuron-1 shRNA cDNA (1.5 μg; white bars) after administration of the $A_{2A}R$ agonist CGS 21680 (CGS, 100 nM), the D_2R agonist quinpirole (1 μM), or both, in the absence or presence of ionomycin (left and right graphs, respectively). Levels of cAMP after CGS alone or after CGS plus quinpirole are expressed as a percentage over basal; cAMP after quinpirole alone are expressed as percentage of decreases with respect to cAMP induced by forskolin (0.5 μM); basal and forskolin-induced cAMP were given as 100% and represented by a dotted line.

In (A), values are expressed as a percentage over basal (100%, dotted line), as means ± SEM of four to six different experiments; one-way ANOVA followed by post hoc Dunnett's multiple comparisons: *$p < 0.05$ and **$p < 0.01$ versus CGS alone. In (B) and (C), values are means ± SEM of four to six different experiments; one-way ANOVA followed by post hoc Dunnett's multiple comparisons: *$p < 0.05$ and **$p < 0.01$ versus CGS 21680 treatment.

the same plasmid under a different promoter (about 10,000 fluorescence units over basal background), and the expression of the NCS-1 shRNA was determined by cotransfection with an empty GFP vector (about 8,000 fluorescence units over basal). Coadministration of CGS 21680 and quinpirole showed a partial or complete negative allosteric modulation between both ligands in the absence or in the presence of ionomycin, respectively (Figure 5B, black bars). This was equivalent to the negative allosteric modulation of $A_{2A}R$ and D_2R ligands demonstrated in transfected HEK293T cells. In fact, the complete negative allosteric modulation was observed in the presence of ionomycin (Figure 5B, right panel, black bars), which would be expected to depend on calneuron-1 (see Figure 4A, right panel, white bars). Indeed, tonic blockade of the negative crosstalk by endogenous calneuron-1 could be demonstrated, as silencing its expression led to a complete loss of the allosteric interaction in the presence of ionomycin (Figure 5B, right graph, white bars). Neither blockade of the expression of calneuron-1 in the absence of ionomycin (Figure 5B, left graph, white bars) nor blockade of the expression of NCS-1 in the presence or absence of ionomycin (Figure 5B, gray bars) significantly modified the effect of coadministration of CGS 21680 and quinpirole on ERK1/2 phosphorylation in striatal cells in culture.

CGS 21680 induced cAMP accumulation and quinpirole decreased forskolin-induced cAMP accumulation in the absence or in the presence of ionomycin (Figure 5C, black bars). Furthermore, quinpirole was able to reduce CGS 21680-induced cAMP in the absence or in the presence of ionomycin (Figure 5C, black bars). Thus, CGS 21680 could not significantly decrease the intrinsic efficacy of quinpirole as an inhibitor of AC signaling. Remarkably, the ability of CGS 21680 to fully

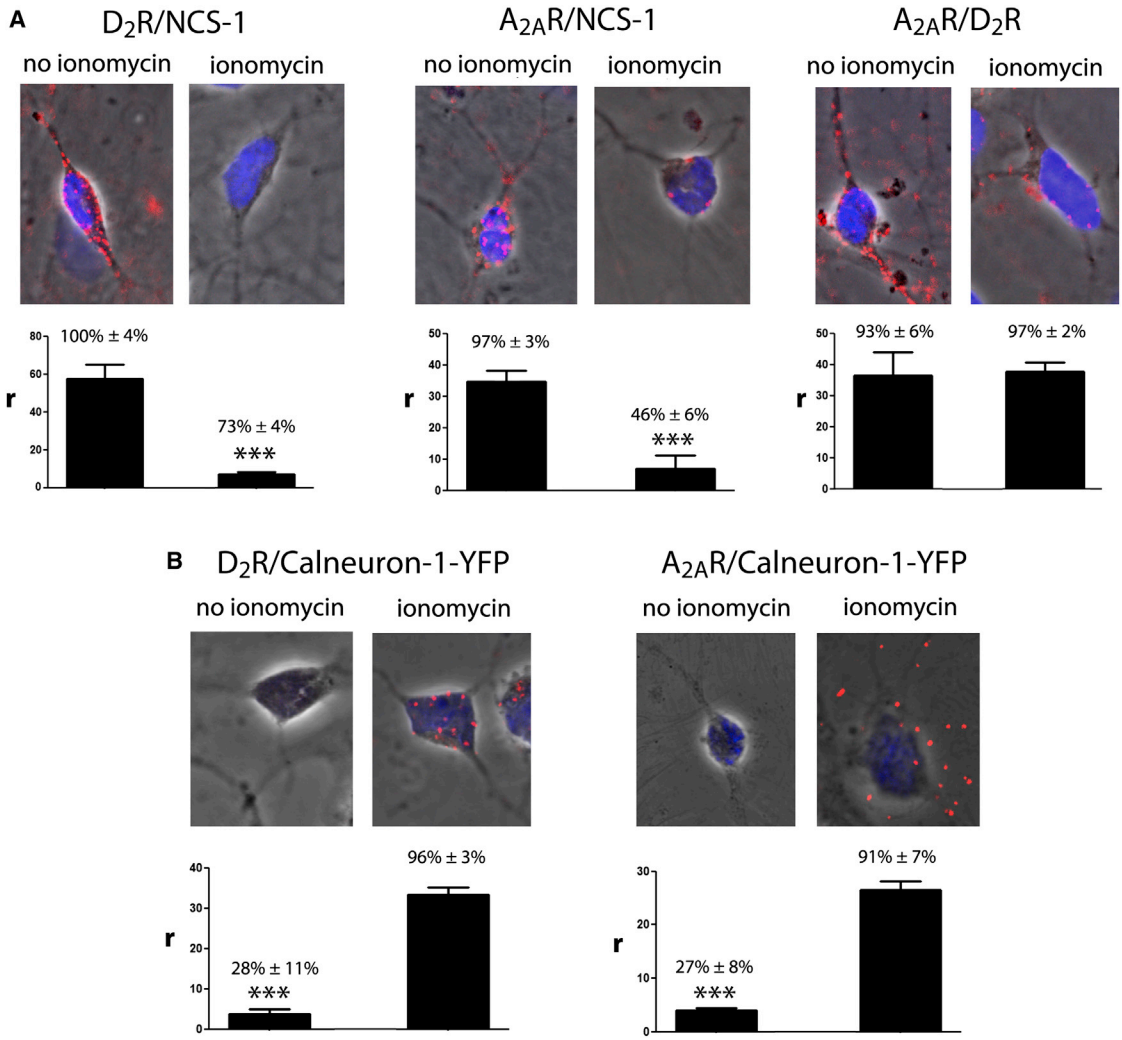

Figure 6. Interactions of NCS-1 and Calneuron-1 with $A_{2A}R$-D_2R Heteromers in Striatal Neurons Depend on Intracellular Ca^{+2} Levels

(A) Proximity ligation assay and confocal microscopy images (superimposed sections) in rat striatal neurons in culture, using primary antibodies for D_2R and NCS-1 (left), $A_{2A}R$ and NCS-1 (middle), and $A_{2A}R$ and D_2R (right), in the absence or presence of ionomycin (1 μM).

(B) PLA and confocal microscopy images (superimposed sections) in rat striatal neurons in culture transfected with calneuron-1-YFP cDNA (1 μg), using primary antibodies for D_2R and YFP (left) and $A_{2A}R$ and YFP (right), in the absence or presence of ionomycin (1 μM). Receptor heteromers and receptor-Ca^{2+}-binding protein complexes appear as red clusters in neurons detected by phase contrast. Cell nuclei were stained with Hoesch (blue). The bar graphs represent PLA quantification: r values represent number of red spots/cell containing spots and percentage values represent the percentage of cells containing one or more red spots respect to the total number of cells. Data (% of positive cells or r) are means ± SEM of counts in 20–30 different neurons of three independent preparations. One-way ANOVA and followed by Bonferroni post hoc test: ***$p < 0.001$ compared with no ionomycin (in A) or ionomicin (in B) of r values.

counteract the inhibitory effect of quinpirole appeared with blockade of the expression of NCS-1 in the absence of ionomycin (Figure 5C, left graph, gray bars) and with blockade of calneuron-1 expression in the presence of ionomycin (Figure 5C, right graph, white bars). These results are in complete agreement with those obtained in HEK293T cells. In striatal cells, however, intracellular Ca^{2+} levels determine which neuronal Ca^{2+}-binding protein interacts with the $A_{2A}R$-D_2R heteromer.

PLA was also used to confirm the ability of Ca^{2+} levels to determine which Ca^{2+}-binding protein interacts with the $A_{2A}R$-D_2R heteromer in striatal neurons. Because of the lack of antibodies sufficiently specific for calneuron-1, only interactions with endogenous NCS-1 could be addressed. D_2R-NCS-1 (Figure 6A, left panels), $A_{2A}R$-NCS-1 (Figure 6A, middle panels), and $A_{2A}R$-D_2R (Figure 6A, left panels) complexes were readily observed in the absence of ionomycin as punctate red spots visualized by phase contrast and with DAPI-stained nuclei. As negative controls, red spots were not observed in the presence of only one of the primary antibodies (Figure S8; NCS-1 KD). The staining was observed in a high percentage of cells (Figure 6A, bar graphs). Although PLA can only assess close proximity between two proteins, the detection of $A_{2A}R$-NCS-1, D_2R-NCS-1, and $A_{2A}R$-D_2R complexes supports that $A_{2A}R$-D_2R-NCS-1 complexes are expressed in the same striatal neurons at low Ca^{2+} levels. Importantly, in the presence of ionomycin, red spots were only observed for $A_{2A}R$-D_2R complexes (Figure 6A, right

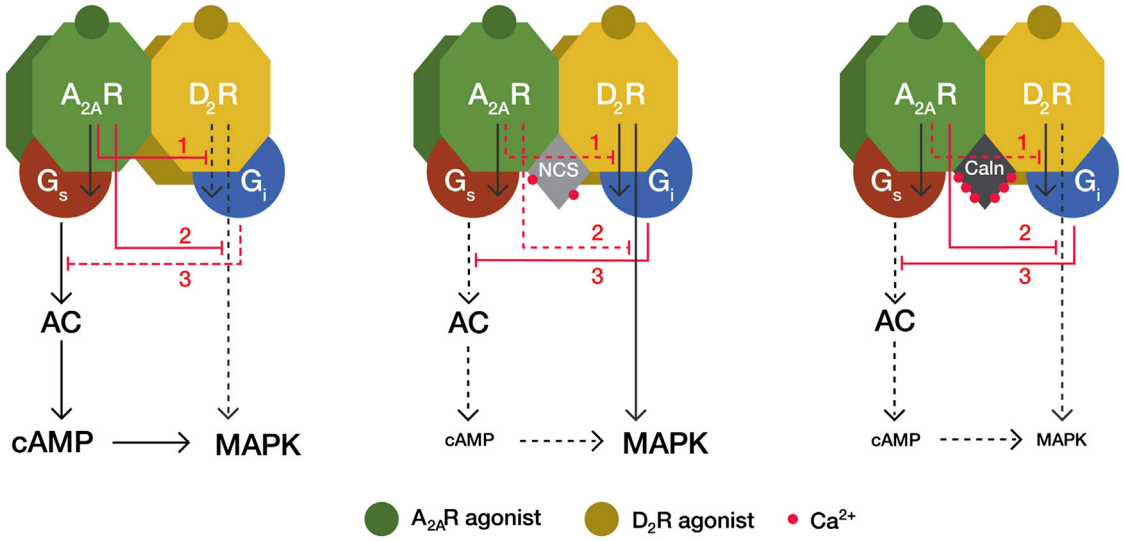

Figure 7. Model Representing the Differential Role of NCS-1 and Calneuron-1 in $A_{2A}R$-D_2R Heteromer Signaling

Depending on the intracellular Ca^{+2} levels, the neuronal Ca^{+2}-binding proteins NCS-1 (NCS) and calneuron-1 (Caln) exert a differential modulation of $A_{2A}R$-D_2R heteromer signaling. In the absence of Ca^{+2}-binding proteins, the D_2R agonist cannot counteract the ability of the $A_{2A}R$ agonist to induce cAMP accumulation (3), due to an allosteric modulation by which $A_{2A}R$ activation inhibits D_2R-mediated G protein-dependent signaling (1). Under these conditions, $A_{2A}R$ activation also inhibits the D_2R agonist-mediated G protein-independent MAPK activation (2). These two allosteric modulations (1 and 2) are absent when NCS-1 binds to the receptor heteromer in the presence of low intracellular Ca^{+2} levels. Under these conditions, coactivation of both receptors in the heteromer does not produce cAMP accumulation, but still induces MAPK activation. When calneuron-1 binds to $A_{2A}R$-D_2R heteromer, the allosteric modulation at the level of G protein-dependent signaling (1) is selectively disrupted and the allosteric modulation at the level of G protein-independent signaling (2) is maintained. This results in very low activation of both MAPK signaling and cAMP production upon coactivation of both receptors in the heteromer, since $A_{2A}R$ agonist-mediated MAPK activation (which is dependent on AC signaling) is also inhibited (3).

panels), and not for D_2R-NCS-1 (Figure 6A, left panels) or $A_{2A}R$-NCS-1 (Figure 6A, middle panels) complexes. To determine whether high Ca^{2+} levels promote calneuron-1 binding to the heteromer, and circumventing the lack of specific calneuron-1 antibodies suitable for PLA, we transfected calneuron-1-YFP and used a specific anti-YFP antibody. $A_{2A}R$-calneuron-1-YFP and D_2R-calneuron-1-YFP complexes could be readily observed by PLA in the presence, but not in the absence, of ionomycin (Figure 6B). The staining was observed in a high percentage of cells only in the presence of ionomycin (Figures 6B, bar graphs). These results from PLA experiments are in complete agreement with low and high Ca^{2+} levels promoting NCS-1 and calneuron-1 binding to the $A_{2A}R$-D_2R heteromer, respectively.

DISCUSSION

The present results provide general findings about the physiological modulation of GPCR heteromer function. First, they demonstrate that in neurons, different Ca^{+2} levels can determine the binding of different neuronal Ca^{+2}-binding proteins to a GPCR heteromer. Second, they demonstrate that the binding of different neuronal Ca^{+2}-binding proteins can promote or disrupt different allosteric modulations in a GPCR heteromer. Third, we show that these differential effects allow a selective modulation of specific GPCR heteromer-dependent signaling pathways.

The strikingly similar results of signaling experiments obtained from HEK293T transfected cells and striatal cells in culture allows us to formulate an heuristic model, which encapsulates previous biochemical findings in the frame of the heteromer, such as a canonical antagonistic G_s-G_i interaction at the level of AC signaling between $A_{2A}R$ and D_2R (Kull et al., 1999; Hillion et al., 2002; Kudlacek et al., 2003), a predominant G protein-cAMP-PKA-dependent $A_{2A}R$-mediated MAPK activation (present results and Klinger et al., 2002; Canals et al., 2005) and a predominant G protein independent MAPK activation mediated by D_2R when coexpressed with $A_{2A}R$ (Huang et al., 2013). Finally, the model assumes the recently proposed tetrameric structure of receptor heteromers (Ferré et al., 2014; Guitart et al., 2014).

The model proposes two independent $A_{2A}R$-mediated inhibitions of two different D_2R-mediated signaling pathways: MAPK activation (G protein independent) and AC inhibition (G protein dependent) (Figure 7). Accumulation of cAMP only occurs upon single or predominant activation of the $A_{2A}R$ in the heteromer, i.e., with low concentrations of dopamine. Under these conditions, the well-known $A_{2A}R$-agonist mediated decrease of the affinity of D_2R agonists counteracts any D_2R-mediated signaling through the heteromer, including AC inhibition. Coactivation with high concentrations of dopamine or D_2R-specific agonists should surmount the decrease in affinity induced by $A_{2A}R$ agonists and allow D_2R agonists to inhibit AC activity. However, in HEK293T transfected cells in the absence of Ca^{+2}-binding proteins, coactivation of both receptors produced similar cAMP levels than those promoted by the $A_{2A}R$ agonist, indicating that it is also possible to observe an $A_{2A}R$ agonist-induced allosteric modulation of the intrinsic efficacy of D_2R agonists (Figure 7, left panel). This modulation, nevertheless, is disrupted with low and high Ca^{+2} levels in the presence of NCS-1 and calneuron-1, respectively, and the modulation is absent in striatal neurons in culture with low or high intracellular Ca^{+2} levels (because of the

endogenous binding of NCS-1 or calneuron-1, respectively). Low levels of cAMP are then produced upon coactivation of the heteromer under these conditions (Figure 7, middle and right panels). Low Ca^{+2} levels (with NCS-1 binding), but not high Ca^{+2} levels (with calneuron-1 binding), disrupt the $A_{2A}R$-mediated negative crosstalk of the D_2R-mediated MAPK activation (Figure 7, middle and right panels). In summary, the allosteric modulation mediated by neuronal Ca^{+2}-binding proteins determines that in the $A_{2A}R$-D_2R heteromer a preferential activation of $A_{2A}R$ leads to both cAMP accumulation and MAPK signaling; upon coactivation of $A_{2A}R$ and D_2R, the presence of low intracellular Ca^{+2} levels leads only to MAPK signaling, and at high Ca^{+2} levels, coactivation leads to a very diminished $A_{2A}R$-D_2R heteromer-mediated signaling response.

Previous reports have shown that, depending on the neuronal function under study, coactivation of $A_{2A}R$ and D_2R leads to significant inhibition of $A_{2A}R$ or D_2R-mediated response, indicating the existence of reciprocal interactions between both receptors that modulate different functional responses. In the striatum, stimulation of $A_{2A}R$ counteracts a D_2R agonist-induced inhibitory modulation of NMDA receptor-mediated effects (Azdad et al., 2009; Higley and Sabatini, 2010), which are dependent on an increase in intracellular Ca^{+2} levels. On the other hand, the ability of $A_{2A}R$ to activate AC seems to be normally restrained by a strong tonic inhibitory effect of endogenous dopamine on striatal D_2R, which efficiently inhibits $A_{2A}R$-mediated AC activation (Svenningsson et al., 1999). To explain the coexistence of these simultaneous reciprocal antagonistic interactions between striatal $A_{2A}R$ and D_2R, we previously postulated their mediation by two different populations of $A_{2A}R$, forming and not forming heteromers with D_2R (Ferré et al., 2011). The present results allow understanding the coexistence of these interactions considering only one predominant population of $A_{2A}R$, which forms heteromers with D_2R. This could account for different G protein-dependent or G protein-independent functional responses, which could be differentially modulated by intracellular Ca^{+2} levels. Apart from adenosine and dopamine, the Ca^{+2}-dependent modulation of $A_{2A}R$-D_2R heteromer function allows further integration of other neurotransmitter systems such as glutamate (through NMDA receptor activation) and acetylcholine (through G_q-coupled muscarinic receptors) (Tozzi et al., 2011).

SIGNIFICANCE

The present study demonstrates that GPCR heteromers are cellular devices that provide a very elaborate integration and modulation of signals from different neurotransmitters that ultimately depends on physiological factors such as intracellular Ca^{+2} levels. Ca^{+2} levels, through different Ca^{+2}-binding proteins, determine functional selectivity within the $A_{2A}R$-D_2R heteromer, which is an important target for the treatment of Parkinson's disease and other neuropsychiatric disorders.

EXPERIMENTAL PROCEDURES

Vectors, Fusion Proteins, and Mutant Proteins

The cDNA constructs encoding human $A_{2A}R$, D_2R, $D_{2\ s}R$, or calmodulin in pcDNA3 vectors were subcloned in pEYFP-N1(enhanced yellow variant of GFP; Clontech, Heidelberg, Germany), pRluc-N1 (PerkinElmer, Wellesley, MA), or pGFP-2-N1 (Biosignal) vectors as previously described (Navarro et al., 2009) to generate $A_{2A}R$-YFP, $A_{2A}R$-Rluc, $A_{2A}R$-GFP^2, D_2R-YFP, D_2R-Rluc, $D_{2\ s}R$-Rluc, or D_2R-GFP^2 fusion proteins. cDNA constructs encoding NCS-1 or caldendrin in pcDNA3 vectors were subcloned in pEYFP-N1 or in pGFP-2-N1 vectors as previously described (Navarro et al., 2012) to generate NCS-1-YFP, caldendrin-YFP, or NCS-1-GFP^2 fusion proteins. The cDNA for calneuron, cloned into pcDNA3.1, was amplified without its stop codons using sense and antisense primers harboring unique BamHI and HindII sites to clone calneuron-1 in pcDNA3.1RLuc vector or HindIII and BamHI to clone in pEYFP-N1 vector or to clone in pGFP-2-N1 vector. The amplified fragments were subcloned to be in-frame with restriction sites of the corresponding vectors to give the plasmids that express calneuron-1-RLuc, calneuron-1-YFP, or calneuron-1-GFP^2. The sequence ^{199}RIFLAARRQ^{207} in the cytoplasm at the end of TM5 of human $A_{2A}R$ was mutated to ^{199}RIFLAAAAQ^{207} to obtain the $A_{2A}R^{A205\text{-}A206}$ as previously described (Navarro et al., 2010). The $D_2R^{428\text{-}443}$ was generated by deletion of the last 16 amino acids from the D_2R and subcloned harboring EcoRI and KpnI restriction sites in pRluc-N1. Calneuron-1 construct truncated in the C terminus (calneuron-1ΔCT) and N-terminal myristoylation-deficient NCS-1 mutant in which YFP is fused to the N terminus of NCS-1 were obtained as described elsewhere (Hradsky et al., 2011). Fusion proteins corresponding to mutant proteins were obtained following the methodology above described.

Primary Cultures of Rat Striatal Neurons, Cell Lines, and Transfection

Primary cultures of striatal neurons were obtained from fetal Sprague Dawley rats of 19 days. Striatal cells were isolated as described in Hradsky et al. (2013) and plated at a confluence of 40,000 cells/0.32 cm^2. Cells were grown in Neurobasal medium supplemented with 2 mM L-glutamine, 100 U/ml penicillin/streptomycin, and 2% (v/v) B27 supplement (GIBCO) in a 96-well plate for 12 days. HEK293T cells were grown in Dulbecco's modified Eagle's medium (DMEM) supplemented with 2 mM L-glutamine, 100 U/ml penicillin/streptomycin, and 5% (v/v) heat inactivated fetal bovine serum (Invitrogen). Primary cultures or HEK293T cells were cultured in the corresponding growth medium in the absence of ionomycin or in the presence of 1 μM of ionomycin. Striatal neurons and HEK293T cells were transfected with the plasmids encoding receptors and/or calcium binding proteins by the PEI (PolyEthylenImine) method as previously described (Carriba et al., 2008).

Resonance Energy Transfer Experiments

Resonance energy transfer experiments are described in other studies (Carriba et al., 2008; Navarro et al., 2009, 2010, 2012), in figure legends, and in Supplemental Information.

Surface Plasmon Resonance

Surface plasmon resonance measurements were performed on a Biacore X100 system (GE Healthcare) to determine the interaction of calcium binding proteins with GST coupled to $A_{2A}R$ third intracellular loop (GST-$A_{2A}R$-IL3) or with D_2R C-terminal domain peptide (P14416, pos. 432-443, peptide purchased from PSL) coupled to a CM5 sensor chip according to the manufacturer's protocol (D_2R-Cterm). Surface plasmon resonance is described in other studies (Catimel et al., 1997; Mikhaylova et al., 2009) and in figure legends (Figure S2).

Immunocytochemistry

Immunocytochemistry assays were performed as previously described (Navarro et al., 2009) using the primary antibodies mouse anti-$A_{2A}R$ (1/200; Millipore) or mouse anti-D_2R (1/200; Santa Cruz Biotechnology) and stained with the secondary antibodies Cy3 anti-mouse (1/200; Jackson ImmunoResearch). NCS-1, calneuron-1, or caldendrin fused to YFP protein were detected by its fluorescence properties. Samples were observed in a Leica SP2 confocal microscope (Leica Microsystems).

Knockdown Endogenous Calneuron-1 or NCS-1 in Primary Cultures of Rat Striatal Neurons

Primary striatal neurons growing in six-well dishes were transfected with the PEI method to knock down the NCS-1 or calneuron-1 expression using

calneuron-1 shRNAII (1xconstruct #2; genecopoeia) with psi-HIV-H1 backbone and eGFP as a marker or pSuper-NCS-1 vector. Cells were incubated for 6–8 hr with the cDNA and the PEI (5.47 mM in nitrogen residues) and 150 mM in NaCl in serum-starved medium. After 6–8 hr, the medium was replaced with a complete culture medium. Forth-eight hours after transfection, the GFP^2 fluorescence signal was detected to test the transfection efficiency. Striatal neurons were then detached and calneuron-1 and NCS-1 expression was detected by western blotting (see Results).

Cell Signaling

The cAMP concentration was determined by homogeneous time-resolved fluorescence (HTRF) energy transfer assay. Lance Ultra cAMP kit (PerkinElmer), based on a europium chelate-labeled cAMP tracer, was used. Cells (4,000 cells/well for transfected HEK293T cells or 6,000 cells/well for primary cultures of striatal neurons) were stimulated with agonists for 15 min in serum-starved DMEM medium supplemented with 50 μM zardeverine, 5 mM HEPES, and 0.1% BSA with or without 1 μM ionomycin, before adding 0.5 μM forskolin or vehicle, and incubating for an additional 15 min period. Fluorescence at 665 nm was analyzed on a PHERAstar Flagship microplate reader equipped with an HTRF optical module (BMG Labtechnologies). ERK 1/2 phosphorylation was determined using the AlphaScreen SureFire kit (Perkin Elmer) following the instructions of the supplier and using an EnSpire Multimode Plate Reader (PerkinElmer). Cells (30,000 cells/well for transfected HEK293T cells or 40,000 cells/well for primary cultures) were seeded in white ProxiPlate 384-well microplates, pretreated at 25°C for 20 min with vehicle or antagonists in serum-starved DMEM medium supplemented or with 1 μM ionomycin and stimulated for an additional 7 min with the indicated agonists.

Proximity Ligation Assays

Heteromers were detected using the Duolink II in situ PLA detection Kit (OLink; Bioscience) following the instructions of the supplier. Primary cultures of striatal neurons were grown on glass coverslips and were fixed in 4% paraformaldehyde for 15 min, washed with PBS containing 20 mM glycine to quench the aldehyde groups, permeabilized with the same buffer containing 0.05% Triton X-100 for 5 min, and successively washed with PBS. After 1 hr incubation at 37°C with the blocking solution in a preheated humidity chamber, primary cultures were incubated overnight in the antibody diluent medium with a mixture of equal amounts of mouse monoclonal anti-$A_{2A}R$ antibody (1:200, Millipore) and the goat polyclonal anti-D_2R antibody (1:200, Santa Cruz) to detect $A_{2A}R$-D_2R heteromers, with the goat polyclonal anti-D_2R antibody and a polyclonal rabbit anti-NCS-1 antibody (1:200, FL190, Santa Cruz) to detect D_2R-NCS-1 complexes, with mouse monoclonal anti-$A_{2A}R$ antibody and the rabbit polyclonal anti-NCS-1 antibody to detect $A_{2A}R$-NCS-1 complexes, with goat polyclonal anti-D_2R antibody and rabbit anti-GFP antibody (1/200, Molecular Probes) to detect D_2R-calneuron-1-YFP complexes or mouse monoclonal anti-$A_{2A}R$ antibody, and rabbit anti-GFP antibody to detect $A_{2A}R$-calneuron-1-YFP complexes. Cells were processed using the PLA probes detecting mouse and goat antibodies (Duolink II PLA probe anti-Mouse plus and Duolink II PLA probe anti-Goat minus), goat and rabbit antibodies (Duolink II PLA probe anti-Goat plus and Duolink II PLA probe anti-Rabbit minus), or mouse and rabbit antibodies (Duolink II PLA probe anti-Mouse plus and Duolink II PLA probe anti-Rabbit minus) diluted in the antibody diluent to a concentration of 1:5. Ligation and amplification were done as indicated by the supplier, and cells were mounted using the mounting medium with Hoechst (1/200; Sigma). Samples were observed in a Leica SP2 confocal microscope (Leica Microsystems) equipped with an apochromatic 63X oil-immersion objective (N.A. 1.4) and 405 nm and a 561 nm laser lines. For each field of view, a stack of two channels (one per staining) and four to eight Z stacks with a step size of 1 μm were acquired. A quantification of cells containing one or more red spots versus total cells (blue nucleus) and, in cells containing spots, the ratio r (number of red spots/cell) were determined considering a total of 25–40 cells from 10–20 different fields using the ImageJ confocal program. Nuclei and red spots were counted on the maximum projections of each image stack. One-way ANOVA followed by Dunet's post hoc multiple comparison test was used to compare the values (% of positive cells or r spots/cell) obtained for each pair of receptors.

SUPPLEMENTAL INFORMATION

Supplemental Information includes Supplemental Experimental Procedures and six figures and can be found with this article online at http://dx.doi.org/10.1016/j.chembiol.2014.10.004.

AUTHOR CONTRIBUTIONS

G.N., M.M., M.R.K., A.C., J.M., V.C., C.L., E.I.C., P.J.M., and S.F. contributed to research design. G.N., D.A., E.M., J.H., P.P.R., and M.M. contributed to experiments. G.N., D.A., E.M., J.H., P.P.R., M.M., C.L., P.J.M., and S.F. contributed to data analysis. G.N., M.M., C.L., P.J.M., and S.F. contributed to the writing of the manuscript.

ACKNOWLEDGMENTS

This work was supported by the intramural funds of the National Institute on Drug Abuse, from the Spanish "Ministerio de Ciencia y Tecnología" (SAF2011-23813), the Government of Catalonia (2009-SGR-12), CIBERNED (CB06/05/0064), the German Research Foundation (SFB779/TPB8, DFG Kr1879/3-1), the Leibniz Foundation (Pakt f. Forschung), a European Molecular Biology Organization Long-Term Fellowship (to M.M., EMBO ALTF 884-2011), the European Commission (EMBOCOFUND2010, GA-2010-267146), a Marie Curie Actions (Intra-European Fellowship), and a "Ramón y Cajal" Fellowship (to P.J.M.).

Received: August 13, 2014
Revised: October 3, 2014
Accepted: October 6, 2014
Published: November 6, 2014

REFERENCES

Azdad, K., Gall, D., Woods, A.S., Ledent, C., Ferré, S., and Schiffmann, S.N. (2009). Dopamine D2 and adenosine A2A receptors regulate NMDA-mediated excitation in accumbens neurons through A2A-D2 receptor heteromerization. Neuropsychopharmacology *34*, 972–986.

Canals, M., Angulo, E., Casadó, V., Canela, E.I., Mallol, J., Viñals, F., Staines, W., Tinner, B., Hillion, J., Agnati, L., et al. (2005). Molecular mechanisms involved in the adenosine A and A receptor-induced neuronal differentiation in neuroblastoma cells and striatal primary cultures. J. Neurochem. *92*, 337–348.

Carriba, P., Navarro, G., Ciruela, F., Ferré, S., Casadó, V., Agnati, L., Cortés, A., Mallol, J., Fuxe, K., Canela, E.I., et al. (2008). Detection of heteromerization of more than two proteins by sequential BRET-FRET. Nat. Methods *5*, 727–733.

Catimel, B., Nerrie, M., Lee, F.T., Scott, A.M., Ritter, G., Welt, S., Old, L.J., Burgess, A.W., and Nice, E.C. (1997). Kinetic analysis of the interaction between the monoclonal antibody A33 and its colonic epithelial antigen by the use of an optical biosensor. A comparison of immobilisation strategies. J. Chromatogr. A *776*, 15–30.

Ferré, S., von Euler, G., Johansson, B., Fredholm, B.B., and Fuxe, K. (1991). Stimulation of high-affinity adenosine A2 receptors decreases the affinity of dopamine D2 receptors in rat striatal membranes. Proc. Natl. Acad. Sci. USA *88*, 7238–7241.

Ferré, S., Baler, R., Bouvier, M., Caron, M.G., Devi, L.A., Durroux, T., Fuxe, K., George, S.R., Javitch, J.A., Lohse, M.J., et al. (2009). Building a new conceptual framework for receptor heteromers. Nat. Chem. Biol. *5*, 131–134.

Ferré, S., Woods, A.S., Navarro, G., Aymerich, M., Lluís, C., and Franco, R. (2010). Calcium-mediated modulation of the quaternary structure and function of adenosine A2A-dopamine D2 receptor heteromers. Curr. Opin. Pharmacol. *10*, 67–72.

Ferré, S., Quiroz, C., Orru, M., Guitart, X., Navarro, G., Cortés, A., Casadó, V., Canela, E.I., Lluis, C., and Franco, R. (2011). Adenosine A(2A) Receptors and A(2A) Receptor heteromers as key players in striatal function. Front. Neuroanat. *5*, 36.

Ferré, S., Casadó, V., Devi, L.A., Filizola, M., Jockers, R., Lohse, M.J., Milligan, G., Pin, J.P., and Guitart, X. (2014). G protein-coupled receptor oligomerization revisited: functional and pharmacological perspectives. Pharmacol. Rev. *66*, 413–434.

Guitart, X., Navarro, G., Moreno, E., Yano, H., Cai, N.S., Sanchez, M., Kumar-Barodia, S., Naidu, Y., Mallol, J., Cortes, A., et al. (2014). Functional selectivity of allosteric interactions within GPCR oligomers: the dopamine D_1-D_3 receptor heterotetramer. Mol. Pharmacol. *86*, 417–429.

Higley, M.J., and Sabatini, B.L. (2010). Competitive regulation of synaptic Ca2+ influx by D2 dopamine and A2A adenosine receptors. Nat. Neurosci. *13*, 958–966.

Hillion, J., Canals, M., Torvinen, M., Casado, V., Scott, R., Terasmaa, A., Hansson, A., Watson, S., Olah, M.E., Mallol, J., et al. (2002). Coaggregation, cointernalization, and codesensitization of adenosine A2A receptors and dopamine D2 receptors. J. Biol. Chem. *277*, 18091–18097.

Hradsky, J., Raghuram, V., Reddy, P.P., Navarro, G., Hupe, M., Casado, V., McCormick, P.J., Sharma, Y., Kreutz, M.R., and Mikhaylova, M. (2011). Post-translational membrane insertion of tail-anchored transmembrane EF-hand Ca2+ sensor calneurons requires the TRC40/Asna1 protein chaperone. J. Biol. Chem. *286*, 36762–36776.

Hradsky, J., Mikhaylova, M., Karpova, A., Kreutz, M.R., and Zuschratter, W. (2013). Super-resolution microscopy of the neuronal calcium-binding proteins Calneuron-1 and Caldendrin. Methods Mol. Biol. *963*, 147–169.

Huang, L., Wu, D.D., Zhang, L., and Feng, L.Y. (2013). Modulation of A_2a receptor antagonist on D_2 receptor internalization and ERK phosphorylation. Acta Pharmacol. Sin. *34*, 1292–1300.

Kabbani, N., Negyessy, L., Lin, R., Goldman-Rakic, P., and Levenson, R. (2002). Interaction with neuronal calcium sensor NCS-1 mediates desensitization of the D2 dopamine receptor. J. Neurosci. *22*, 8476–8486.

Klinger, M., Kudlacek, O., Seidel, M.G., Freissmuth, M., and Sexl, V. (2002). MAP kinase stimulation by cAMP does not require RAP1 but SRC family kinases. J. Biol. Chem. *277*, 32490–32497.

Kudlacek, O., Just, H., Korkhov, V.M., Vartian, N., Klinger, M., Pankevych, H., Yang, Q., Nanoff, C., Freissmuth, M., and Boehm, S. (2003). The human D2 dopamine receptor synergizes with the A2A adenosine receptor to stimulate adenylyl cyclase in PC12 cells. Neuropsychopharmacology *28*, 1317–1327.

Kull, B., Ferré, S., Arslan, G., Svenningsson, P., Fuxe, K., Owman, C., and Fredholm, B.B. (1999). Reciprocal interactions between adenosine A2A and dopamine D2 receptors in Chinese hamster ovary cells co-transfected with the two receptors. Biochem. Pharmacol. *58*, 1035–1045.

Mikhaylova, M., Reddy, P.P., Munsch, T., Landgraf, P., Suman, S.K., Smalla, K.H., Gundelfinger, E.D., Sharma, Y., and Kreutz, M.R. (2009). Calneurons provide a calcium threshold for trans-Golgi network to plasma membrane trafficking. Proc. Natl. Acad. Sci. USA *106*, 9093–9098.

Mikhaylova, M., Hradsky, J., and Kreutz, M.R. (2011). Between promiscuity and specificity: novel roles of EF-hand calcium sensors in neuronal Ca2+ signalling. J. Neurochem. *118*, 695–713.

Navarro, G., Aymerich, M.S., Marcellino, D., Cortés, A., Casadó, V., Mallol, J., Canela, E.I., Agnati, L., Woods, A.S., Fuxe, K., et al. (2009). Interactions between calmodulin, adenosine A2A, and dopamine D2 receptors. J. Biol. Chem. *284*, 28058–28068.

Navarro, G., Ferré, S., Cordomi, A., Moreno, E., Mallol, J., Casadó, V., Cortés, A., Hoffmann, H., Ortiz, J., Canela, E.I., et al. (2010). Interactions between intracellular domains as key determinants of the quaternary structure and function of receptor heteromers. J. Biol. Chem. *285*, 27346–27359.

Navarro, G., Hradsky, J., Lluís, C., Casadó, V., McCormick, P.J., Kreutz, M.R., and Mikhaylova, M. (2012). NCS-1 associates with adenosine A(2A) receptors and modulates receptor function. Front. Mol. Neurosci. *5*, 53.

Saab, B.J., Georgiou, J., Nath, A., Lee, F.J., Wang, M., Michalon, A., Liu, F., Mansuy, I.M., and Roder, J.C. (2009). NCS-1 in the dentate gyrus promotes exploration, synaptic plasticity, and rapid acquisition of spatial memory. Neuron *63*, 643–656.

Svenningsson, P., Fourreau, L., Bloch, B., Fredholm, B.B., Gonon, F., and Le Moine, C. (1999). Opposite tonic modulation of dopamine and adenosine on c-fos gene expression in striatopallidal neurons. Neuroscience *89*, 827–837.

Tozzi, A., de Iure, A., Di Filippo, M., Tantucci, M., Costa, C., Borsini, F., Ghiglieri, V., Giampà, C., Fusco, F.R., Picconi, B., and Calabresi, P. (2011). The distinct role of medium spiny neurons and cholinergic interneurons in the D_2/A_2A receptor interaction in the striatum: implications for Parkinson's disease. J. Neurosci. *31*, 1850–1862.

Trifilieff, P., Rives, M.L., Urizar, E., Piskorowski, R.A., Vishwasrao, H.D., Castrillon, J., Schmauss, C., Slättman, M., Gullberg, M., and Javitch, J.A. (2011). Detection of antigen interactions ex vivo by proximity ligation assay: endogenous dopamine D2-adenosine A2A receptor complexes in the striatum. Biotechniques *51*, 111–118.

